Soft Matter

PAPER

Cite this: *Soft Matter*, 2019, **15**, 3248

Chemotaxis mediated interactions can stabilize the hydrodynamic instabilities in active suspensions

Mehrana R. Nejad[a] and Ali Najafi *[ab]

Received 10th January 2019,
Accepted 18th March 2019

DOI: 10.1039/c9sm00058e

rsc.li/soft-matter-journal

Ordered phases in active suspensions of polar swimmers are under long-wavelength hydrodynamic mediated instabilities. In this article, we show that chemical molecules dissolved in aqueous suspensions, as an unavoidable part of most wet active systems, can mediate long-range interactions and subsequently stabilize the polar phase. Chemoattractants in living suspensions and dissolved molecules in synthesized Janus suspensions are reminiscent of such chemical molecules. Communication between swimmers through the gradients of such chemicals is the foundation of this stabilization mechanism. To classify the stable states of such active systems, we investigate the detailed phase diagrams for two classes of systems with momentum conserving and non-conserving dynamics. Our linear stability analysis shows that the proposed stabilization mechanism can work for swimmers with different dynamical properties, *e.g.*, pushers or pullers and with various static characteristics, *e.g.*, spherical, oblate or prolate geometries.

1 Introduction

Understanding and explaining the physics of active matter have attracted much interest recently.[1,2,4,5] Active suspensions, both living and synthetic systems, are not bound by equilibrium laws, and thus show a variety of behaviors ranging from collective self-organized motion (even in two dimension)[6–8] to nontrivial rheological properties.[9–13] Long-range rotational order observed in active suspensions is under strong dynamical instabilities mediated by hydrodynamic interactions in low Reynolds wet systems.[6,14] This instability is generic in the sense that it is not affected by any short-range interaction but its underlying mechanism is very sensitive to the hydrodynamic details of individual swimmers. For pushers (pullers), bend (splay) fluctuations diverge and initiate the instability. Interestingly and in contrast to this hydrodynamic mediated instability, there are examples where ordered phases can be observed experimentally. Furthermore, studying stabilization mechanisms provides guidelines for designing microswimmers exhibiting collective ordered motion. System-size-dependent fluctuations in elastic systems[15] and 2-D film confinement[16,17] provide mechanisms that can stabilize the polar phase.

In this article, we show that chemical signaling between swimmers is a potential mechanism that can stabilize the polar phase. The phenomenon of chemotaxis, which is a vital activity in most living organisms,[18] and also the phoretic interactions between active agents in suspensions of artificial swimmers[19,21] can be considered as examples of such chemical signaling. Depending on the details of the system under investigation, chemotaxis itself can initiate Keller–Segel type instabilities[22,23] but there are examples showing that phoretic interactions between active agents can lead to interesting collective behaviors.[19,20,24,25] In these references, hydrodynamic interaction has not been taken into account and the stability of the polar state has not been studied. In another work,[26] polarization of a Janus particle along a chemical or temperature gradient, which is generated by the particle itself or by other neighbors, has been considered. However, the stability of the polar state and the hydrodynamic interaction between swimmers have not been studied. The interplay between hydrodynamic interaction and chemotaxis was investigated previously with a view on the effects of self-generated flows on the stability of the isotropic phase of auto-chemotactic swimmers.[27] In a different regime and at the threshold of hydrodynamic instabilities, we study the influence of chemotactic interaction on long wave-length instabilities of a polar and isotropic suspension. In both living and synthetic active matter, individual agents change their state of motion in response to a gradient in chemicals. Here we use a macroscopic phenomenological description in which, chemotaxis can be considered as currents proportional to the local gradient of concentration. Although there are microscopic derivations that can support this picture,[23,28] chemotactic coefficients defined in this way can also be considered as parameters

[a] *Department of Physics, Institute for Advanced Studies in Basic Sciences (IASBS), Zanjan 45137-66731, Iran*
[b] *Research Center for Basic Sciences & Modern Technologies (RBST), Institute for Advanced Studies in Basic Sciences, Zanjan, Iran. E-mail: najafi@iasbs.ac.ir*

that can be measured experimentally. Extending the idea of phoretic Brownian particles[29] to both momentum conserving and non-conserving systems, we formulate a continuum description for an active suspension and use linear stability analysis to determine the stability criteria.

The structure of this paper is as follows: in Section 2, we introduce the model and write the basic equations. Fluctuations around steady states and stability of polar and isotropic phases are analyzed in Sections 3 and 4, respectively. Finally, some concluding remarks will be discussed in Section 5.

2 Model and dynamical equations

As shown in Fig. 1, let us consider an interacting suspension of swimmers moving in the presence of a concentration of chemical nutrients. Each swimmer is an axisymmetric particle with major and minor diameters given by ℓ and $\Delta\ell$ and it moves with an intrinsic speed given by v_0 along its major axis denoted by a unit vector $\hat{\mathbf{m}}$. In a mean-field description, the dynamics of this suspension is described by single particle probability distribution function $\psi(\mathbf{r},\hat{\mathbf{m}},t)$, showing the probability to find a swimmer with orientation $\hat{\mathbf{m}}$ in position r at time t. In addition to this distribution function, the chemical concentration $c(\mathbf{r},t)$ and velocity profile of the ambient fluid $\mathbf{u}(\mathbf{r},t)$, created by moving swimmers, are dynamical variables that need to be determined.

A very important step in our modeling is a phenomenological picture that we will use to consider the interaction between the chemical molecules and swimmers. Forgetting the details of the microscopic scenario of the interaction between a swimmer and such chemical molecules, a macroscopic phenomenological model can be used to capture the essence of interaction with chemicals in both cases of bacteria and Janus particles. Both chemotaxis (for bacteria)[23,29] and phoretic (for active Janus particles) types of interactions[28] can be modeled phenomenologically with contributions to the speed of swimmers that are proportional to the local gradient of chemical molecules. In this picture, linear and angular contributions to the velocity of swimmers are given by $-\chi_t\nabla c$ and $-\chi_r\hat{\mathbf{m}}\times\nabla c$, respectively, where χ_t and χ_r are two phenomenological parameters. Both positive and negative values for these parameters are realizable in experiments. Positive (negative) values of $\chi_{t,r}$ correspond to chemo-repellent (-attractant) systems where the source of chemical molecules repel (attract) the swimmers.

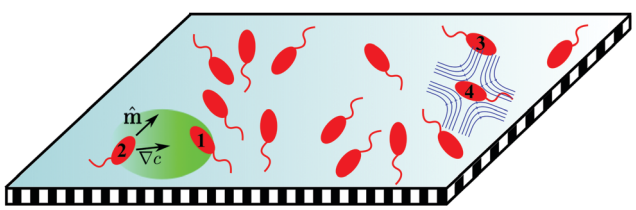

Fig. 1 A schematic view showing a suspension of active swimmers interacting *via* hydrodynamic and chemotaxis mediated interactions. By both flow and chemical gradient produced by a swimmer, the motion of other swimmers can be affected. Flow streamlines produced by a typical pusher swimmer and self-generated gradient of chemical molecules developed around another typical swimmer are shown by blue and green colors, respectively.

The Smoluchowski equation for ψ governs the dynamics of this interacting suspension as:

$$\frac{\partial}{\partial t}\psi(\mathbf{r},\hat{\mathbf{m}},t)+\nabla_m\cdot\mathbf{J}^m+\nabla\cdot\mathbf{J}^t=0, \tag{1}$$

where, ∇ and ∇_m stand for positional gradient and gradient operator on unit sphere, respectively. The current densities are given by:

$$\begin{aligned}\mathbf{J}^m&=(\mathbf{I}-\hat{\mathbf{m}}\hat{\mathbf{m}})\cdot[(\Omega+A\mathbf{G})\cdot\hat{\mathbf{m}}-\chi_r\nabla c]\psi-D_r\nabla_m\psi\\ \mathbf{J}^t&=[\nu_0\hat{\mathbf{m}}+\mathbf{u}-D\nabla-\chi_t\nabla c]\psi.\end{aligned} \tag{2}$$

As one can see, the phenomena of convection (terms proportional to v_0 and $\mathbf{u}$) and diffusion (terms denoted by translational and rotational diffusion tensors, D and D_r) have contributions in current densities. To consider the flow-mediated motion of colloidal objects immersed in a linear flow, the symmetric and antisymmetric parts of the fluid velocity gradient are denoted by $2G=\nabla\mathbf{u}+(\nabla\mathbf{u})^T$ and $2\Omega=\nabla\mathbf{u}-(\nabla\mathbf{u})^T$, respectively. For axisymmetric swimmers we have $A=(1-\Delta^2)/(1+\Delta^2)$.[30]

In terms of the distribution function, we define density ρ, polarization $\mathbf{p}$ and nematic order parameter $\mathbf{Q}$ as

$$\rho=\langle 1\rangle,\ \mathbf{p}=\langle\hat{\mathbf{m}}\rangle,\ \mathbf{Q}=\langle(\hat{\mathbf{m}}\hat{\mathbf{m}}-I/3)\rangle, \tag{3}$$

where, $\langle\times\rangle=\int d\hat{\mathbf{m}}\times\psi$. In the next parts, we will see that instead of the dynamics of the distribution function ψ, we can study the dynamics of these moments. To take into account the hydrodynamic interactions, we consider the dynamics of the ambient fluid. Denoting the viscosity of the fluid by η, fluid flow obeys Stokes and incompressibility equations as

$$\eta\nabla^2\mathbf{u}-\nabla\Pi=\nabla\cdot\sigma^a,\quad \nabla\cdot\mathbf{u}=0. \tag{4}$$

Assuming that the swimmers are force-dipoles with strength ζ, their contribution to the Stokes equations appears as an active stress[2] given by $\sigma^a=\zeta\mathbf{Q}$. For a dipolar swimmer, we assign $\zeta=6\pi\eta\ell^2v_0\Delta_p$, where Δ_p is a dimensionless number showing the strength of the force-dipole associated with swimmers, for pusher $\Delta_p>0$ and for puller $\Delta_p<0$. It should be mentioned that, in addition to the way we are modeling the hydrodynamic interaction, an effective two-body interaction between swimmers can be considered alternatively.[31–34]

Considering both diffusion and convection, the concentration of chemical molecules obeys the following equation:

$$\partial_t c(\mathbf{r},t)=-\mathbf{u}\cdot\nabla c+D_c\nabla^2c-K(c)\rho(\mathbf{r},t)+S, \tag{5}$$

where chemical molecules are injected into the medium through a uniform source term S and swimmers act as sinks for chemical molecules for $K>0$. The uniform source $S>0$ is responsible for developing a steady-state in the system. Reaction rate K is assumed to obey Michaelis–Menten kinetics, characteristic of catalytic reactions as: $K(c)=K_0c(c+c_M)^{-1}$, where K_0 is the maximum reaction rate and c_M denotes a concentration at which the reaction rate reaches its half-maximum value.[35,37,38]

The kinetics we are considering here is the simplest choice and there are other possibilities that we can consider as well without any crucial change in our final results. Considering the fact that the diffusion time scale for chemical molecules is much smaller than the time scale in which swimmers move, we can go to the stationary state limit of the diffusion eqn (5). As a result of this simplification, chemical concentration can be considered as a function of instantaneous positions of the swimmers.[19,29]

To study the dynamics of fluctuations, we consider the case that our system fluctuates around uniform distributions of chemical nutrients and swimmers and we set $c = c_0 + \delta c$ and $\rho = \rho_0 + \delta\rho$. Denoting the fluctuation wave vector by $\mathbf{q} = q\hat{\mathbf{q}}$ and introducing the Fourier transform for any fluctuating field as $f(\mathbf{r},t) = \int d\mathbf{q}d\omega\tilde{f}(\mathbf{q},\omega)e^{i(\mathbf{q}\cdot\mathbf{r}-\omega t)}$, the chemical concentration and fluid velocity profile can be obtained explicitly as:

$$\tilde{\mathbf{u}} = \frac{i\zeta}{\eta q}(\hat{\mathbf{q}}\hat{\mathbf{q}} - \mathbf{I})\cdot\delta\tilde{\mathbf{Q}}\cdot q, \quad \delta\tilde{c} = \frac{-K(c_0)}{D_c q^2 + \rho_0\partial_c K}\delta\tilde{\rho}, \tag{6}$$

where variables with tilde sign show Fourier modes. In terms of chemical concentration, two different regimes of diffusion- and reaction-dominated can be distinguished. For sufficiently small concentrations $c_0 \ll c_M$, the dynamics of chemical molecules is totally governed by the reaction process as $\delta\tilde{c} = -(c_0/\rho_0)\delta\tilde{\rho}$, but for larger concentrations ($c_0 \geq c_M$), it is dominated by diffusion, $\delta\tilde{c} = -(K_0/D_c q^2)\delta\tilde{\rho}$.

The equations governing the dynamics of density, polarization and nematic order parameter are:

$$\begin{aligned}
\partial_t\rho &= -\nabla\cdot(\nu_0\mathbf{p}) + \chi_t\nabla\cdot(\nabla c\rho) + \dot{\rho}^L,\\
\partial_t\mathbf{p}_\alpha &= -\nu_0\partial_i\left(\mathbf{Q}_{i\alpha} + \frac{1}{3}\delta_{i\alpha}\rho\right) - 2D_r\mathbf{p}_\alpha + \chi_t\nabla_\beta\left(\nabla_\beta c\,\mathbf{p}_\alpha\right)\\
&\quad + \chi_r\nabla_\beta c\left(\mathbf{Q}_{\beta\alpha} - \frac{2}{3}\delta_{\alpha\beta}\rho\right) + \dot{\mathbf{p}}^L_\alpha,\\
\partial_t\mathbf{Q}_{\alpha\beta} &= \chi_t\partial_t\left(\partial_t c\mathbf{Q}_{\alpha\beta}\right) - 6D_r\mathbf{Q}_{\alpha\beta} + v_0\partial_\gamma\left(\frac{1}{3}\delta_{\alpha\beta}\mathbf{p}_\gamma - \mathbf{O}_{\gamma\beta\alpha}{}^3\right)\\
&\quad + \dot{\mathbf{Q}}^L_{\alpha\beta} + 2\chi_r\left(\partial_t c\mathbf{O}_{\alpha\beta\iota}{}^3 - \mathbf{p}_\alpha\nabla_\beta c - \mathbf{p}_\beta\nabla_\alpha c\right),
\end{aligned} \tag{7}$$

where terms denoted by superscripts L show the contributions that are due to the long-range hydrodynamic interactions:

$$\begin{aligned}
\dot{\rho}^L &= -\mathbf{u}(\mathbf{r},t)\cdot\nabla\rho(\mathbf{r},t),\\
\dot{\mathbf{p}}^L_\alpha &= A\left(\delta_{\alpha\iota}\mathbf{p}_\beta - \mathbf{O}_{\alpha\beta\iota}{}^3\right)\mathbf{G}_{\iota\beta} - \mathbf{u}\cdot\nabla\mathbf{P}_\alpha + \frac{1}{2}\left(\mathbf{P}\cdot\nabla\mathbf{u}_\alpha - \mathbf{p}_\beta\nabla_\alpha\mathbf{u}_\beta\right),\\
\dot{\mathbf{Q}}^L_{\alpha\beta} &= -\mathbf{u}\cdot\nabla Q_{\alpha\beta} - 2A\mathbf{O}_{\alpha\beta\gamma\iota}{}^4\mathbf{G}_{\gamma\iota} + A\mathbf{G}_{\alpha\iota}\left(Q_{\iota\beta} + \frac{\delta_{\iota\beta}\rho}{3}\right)\\
&\quad + A\left(Q_{\iota\alpha} + \frac{\delta_{\iota\alpha}\rho}{3}\right)G_{\iota\beta} + \Omega_{\alpha\iota}\mathbf{Q}_{\iota\beta} - \mathbf{Q}_{\alpha\iota}\Omega_{\iota\beta},
\end{aligned} \tag{8}$$

where higher order moments are defined as: $\mathbf{O}_{\alpha\beta_\gamma}{}^3 = \langle\hat{\mathbf{m}}_\alpha\hat{\mathbf{m}}_\beta\hat{\mathbf{m}}_\gamma\rangle$ and $\mathbf{O}_{\alpha\beta\gamma\nu}{}^4 = \langle\hat{\mathbf{m}}_\alpha\hat{\mathbf{m}}_\beta\hat{\mathbf{m}}_\gamma\hat{\mathbf{m}}_\nu\rangle$.

The model that we have introduced here does not allow any long-range order. This is due to the fact that long-range order will result from short-range interactions, the interactions that are absent in our model. As shown in ref. 34 by introducing an aligning short-range interaction, one can achieve states with order. There is a critical density in the system denoted by ρ^*, beyond which ($\rho_0 > \rho^*$) the system can be in a state with polarization given by $\mathbf{p} = p_0\hat{\mathbf{n}}$. For small densities ($\rho_0 < \rho^*$), short-range interactions are not able to induce any polarization and the system is in an isotropic state with uniform density. Critical density ρ^* depends on the strength of short-range interactions. In the following parts, we will assume that as a result of a short-range interaction, such steady-state solutions (polar and homogenous states) exist and ask how such states are stable in the presence of long-range, both hydrodynamic and phoretic interactions.

Before continuing, it is convenient to introduce dimensionless parameters. Frequency, wave number, chemotaxis coefficients and diffusion constants are important parameters that we make dimensionless. In terms of $\gamma = 3\pi\rho_0\ell^3$, $\omega_0 = (\gamma v_0/2\ell)$ and $\chi_0 = (D_c\omega_0/\rho_0 K_0 v_0)$, dimensionless quantities can be defined as:

$$\begin{aligned}
&\bar{\chi}_t = \frac{\chi_t}{2v_0\chi_0}, \bar{\chi}_r = \frac{\chi_r}{\omega_0\chi_0}, \bar{q} = q\ell, \bar{\omega} = \omega/\omega_0,\\
&\bar{D}_r = D_r/\omega_0, \quad \bar{D} = D/\left(\ell^2\omega_0\right), \quad \mathrm{Pe} = v_0\ell/D_c.
\end{aligned} \tag{9}$$

Péclet number Pe is another important parameter that is defined here. This number measures the relative importance of convection and diffusion of chemical molecules in a length scale given by the size of swimmers. It should be noted that in our definition for dimensionless chemotactic coefficients $\bar{\chi}_{t,r}$, both reaction rate K_0 and chemotactic coefficients $\chi_{t,r}$ have a role in determining the sign of dimensionless coefficients $\bar{\chi}_{t,r}$. In fact we will see that for positive $\bar{\chi}_{t,r}$, the effective interaction between swimmers will be attraction while for its negative values the effective interaction will be repulsion.

3 Stability of the polar state

As mentioned before, for a system with density satisfying $\rho_0 > \rho^*$, a polar state can be established. In this polar state, density ρ_0 and polarization denoted by director $\hat{\mathbf{n}}$ are the relevant hydrodynamic variables.[34] To study the stability of this polar phase, we consider fluctuations in the director given by: $\hat{\mathbf{n}} + \delta n$ and study the dynamics of fluctuations. Denoting by θ, the angle between $\hat{\mathbf{q}}$ and $\hat{\mathbf{n}}$, the following linearized equations describe the fluctuations in the polar phase,

$$\begin{aligned}
&-2\rho_0\gamma^{-1}\bar{q}\hat{\mathbf{q}}\cdot\delta\tilde{\mathbf{n}} + \left[\bar{\omega} - 2i\bar{\chi}t - 2\bar{q}\gamma^{-1}\cos\theta\right]\delta\tilde{\rho} = 0\\
&\left[\bar{\omega} - 2\gamma^{-1}\bar{q}\cos\theta - 2i\Delta_p\cos 2\theta A'\right]\rho_0\bar{q}\hat{\mathbf{q}}\cdot\delta\tilde{\mathbf{n}}\\
&\quad + \sin^2\theta\left(\gamma\bar{\chi}_r/2 + 2i\bar{q}\Delta_p\cos\theta A'\right)\delta\tilde{\rho} = 0
\end{aligned} \tag{10}$$

with $A' = (1 + A\cos 2\theta)$. Here we have considered the diffusion-dominated regime for the chemical reactions. It should be mentioned that in bulk systems, chemotactic interaction in the reaction-dominated regime cannot stabilize the polar state. According to the above equations, for a case in which $A \neq 0$, dispersion relation can be written as $\bar{\omega} = 2\gamma^{-1}\bar{q}\cos\theta + ih_\pm'$,

with

$$h_{\pm}{}' = \left[\pm\left(\frac{\sin\theta^2\left(\bar{\chi}_r+4i\gamma^{-1}\Delta_p\cos\theta\bar{q}(1+A\cos\theta)\right)}{g^2}+\left(1-\frac{2\bar{\chi}_t}{g}\right)^2\right)^{\frac{1}{2}}+1\right]g(\theta), \quad (11)$$

where $g(\theta) = \Delta_p \cos 2\theta(1 + A\cos 2\theta) + \bar{\chi}_t$. The condition $\Im(\bar{\omega}) < 0$ ($\Re(\bar{\omega}) \neq 0$ or $= 0$) shows the stability criterion (oscillating or non-oscillating) and the onset of instability is given by the condition $\Im(\bar{\omega}) > 0$. By changing the parameter A, we can study the role of swimmers' geometry in the stability of the polar suspension. A disk-shape swimmer corresponds to $A = -1$ and $A = 1$ stands for a rod-like swimmer.

3.1 Hydrodynamic and chemotactic instabilities

Well-established results corresponding to the hydrodynamic mediated instability of polar phase can be seen by ignoring the chemotaxis in the above results.[2,3,6,39] Setting $\bar{q} = \bar{\chi}_t = \bar{\chi}_r = A = 0$, we see that $\Im(\bar{\omega}) = 2\Delta_p \cos 2\theta$, showing that instability of pushers ($\Delta_p > 0$) and pullers ($\Delta_p < 0$) is due to bend ($\theta = 0$) and splay ($\theta = \pi/2$) fluctuations, respectively. Chemotaxis mediated instabilities in the absence of hydrodynamic interactions can also be investigated by setting $\Delta_p = q = 0$, which will result in $\Im(\bar{\omega}) = \bar{\chi}_t\left[1 \pm \Re\left(1 + \frac{\sin^2\theta\bar{\chi}_r}{\bar{\chi}_t^2}\right)^{\frac{1}{2}}\right]$. Regarding the signs of $\bar{\chi}_r$ and $\bar{\chi}_t$, we can distinguish different cases. When both of them are positive or one positive and the other negative, it is easily seen that the homogeneous polar state is unstable. For $\bar{\chi}_t > 0$, chemotaxis collapse occurs that eventually makes the system inhomogeneous. For $\bar{\chi}_r > 0$, an instability in director (resulted from phoretic torque between swimmers) destroys polar order towards aster formation. Only in the case where both chemotactic coefficients are negative ($\bar{\chi}_r < 0$, $\bar{\chi}_t < 0$) is a stable polar state expected to be observed in the system. In this regime, and for angles satisfying $\bar{\chi}_r \sin^2\theta < -\bar{\chi}_t{}^2$, oscillating states can also be observed. Wave-number dependent oscillations of the polar state in active matter have been studied before.[40,41] In the presence of chemotactic interaction, we showed that in addition to sound-like waves (the first term in $\bar{\omega}$), wave-number independent ($\bar{q} = 0$) oscillations can also be observed.

3.2 The role of chemotaxis

When both chemotaxis and hydrodynamics are considered, interesting results will appear. Regarding the above discussion and in terms of chemotactic coefficients, we expect to see non-trivial results when $\bar{\chi}_r < 0$, $\bar{\chi}_t < 0$. For a fixed and negative value of $\bar{\chi}_t$, Fig. 2 shows a phase diagram of possible phases that can appear in a non-confined interacting suspension at the limit of $\bar{q} = 0$. Chemotactic coefficient $\bar{\chi}_r$ and strength of hydrodynamic interactions Δ_p are used to label the phase diagram.

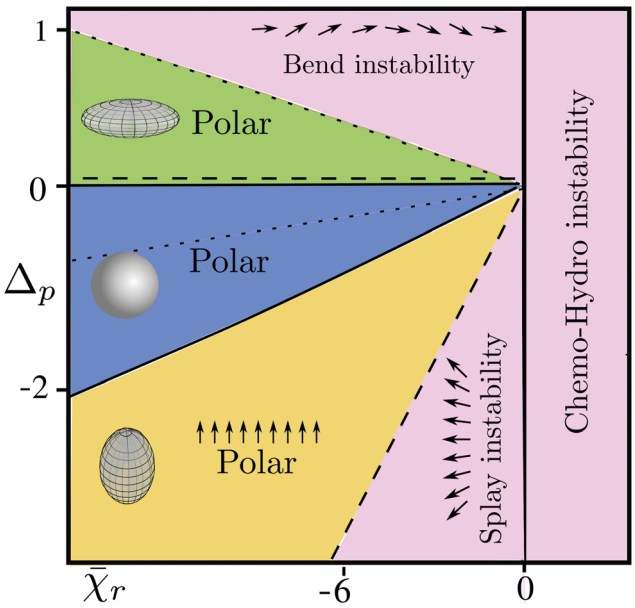

Fig. 2 Stable regions for a 3-D momentum-conserving polar suspension. In terms of Δ_p and $\bar{\chi}_r$, stable regions are shown for different shapes of the swimmers. Boundaries of the stable regions are shown by dotted, solid and dashed lines for disk-shaped, spherical and rod-shaped swimmers, respectively. We set $\bar{\chi}_t = -2.5$.

Eqn (11) shows that for rod-shaped swimmers, bend (splay) fluctuations are stronger (weaker) in pusher (puller) suspensions in comparison to the spherical swimmers. This means that chemotaxis can stabilize the polar phase in a suspension of rod-shaped pullers more easily. For disk-shaped swimmers, splay (bend) fluctuations are stronger (weaker) in suspensions of pullers (pushers) in comparison with spherical swimmers.

For a suspension of spherical swimmers, as seen from the phase diagram in Fig. 2, chemotaxis is not able to completely suppress hydrodynamic instabilities of pushers ($\Delta_p > 0$) in the bulk of a fluid and a polar suspension of pushers is always unstable. Interestingly, chemotaxis can suppress the splay fluctuations and stabilize the polar state for spherical pullers ($\Delta_p < 0$). Both static and oscillating polar phases can be seen at the phase diagram. Oscillations of polar state observed in this phase diagram are scale-free in the sense that their frequencies do not depend on wave-vector. The stable parts of the phase diagram for different swimmer geometries are presented in Fig. 2.

To have an intuitive picture of the stabilization mechanism, Fig. 3(a) and (b) show a collection of nearly parallel spherical swimmers ($A = 0$) that are under small bend and splay fluctuations, respectively. Spherical geometry is chosen here to build a simple intuition. As seen from the figures and as a result of such director distortions, density fluctuations will appear in the system due to the self propulsion of swimmers. In terms of director fluctuations δn, density fluctuation for the case of splay is a first order effect (in terms of fluctuations) but it is second order for bend distortion. In both cases, consideration of density fluctuations shows that reoriented swimmers are more

affected by the swimmers from the left side where their overall chemotactic torque tends to diminish fluctuations. Fluctuation suppression is much stronger for the splay case because density fluctuations are stronger and as a result, chemotactic torque is larger for splay fluctuations. To obtain this result, we have used the relation $-\bar{\chi}_r \hat{\mathbf{m}} \times \nabla c$ with $\bar{\chi}_r < 0$ for chemotactic angular velocity and have assumed that each swimmer produces a radial gradient of chemicals. To prevent chemotactic collapse, it is necessary to consider $\bar{\chi}_{t,r} < 0$. For the case of bend fluctuations and at the first order of δn, chemotactic torques acting on the distorted swimmer from left and right sides cancel each other because density fluctuation created by a bend perturbation is second order in δn. Considering the higher order corrections, chemotaxis tends to diminish the fluctuations, but it is not so strong to remove the instability mediated from bend fluctuations in a system of spherical pushers. As it is clear from Fig. 3, chemotactic interaction can suppress hydrodynamic instabilities for suspensions of disk-shaped pushers. This happens because, in contrast with rod-shaped and spherical pusher suspensions, the growth rate of hydrodynamic instabilities for disk-shaped pushers is weak in small values of the θ and vanishes at $\theta = 0$.

To investigate the stability of the polar state in a system with finite size, we have plotted in Fig. 3(c) and (d) the growth rate $\Im(\omega)$ as a function of θ for different values of $\bar{q}$ for spherical swimmers. Regarding the instability criterion $\Im(\omega) > 0$, Fig. 3(c) shows that for pushers and in the absence of chemotaxis, the instability comes from bend modes ($\theta = 0,\pi$). Here, chemotaxis can suppress the fluctuations and make the unstable angles narrower, but it is not able to totally remove the instability. This conclusion is valid for both infinite and finite systems. Fig. 3(d) shows that for pullers, and at $\bar{\chi}_r = \bar{\chi}_t = 0$, splay modes ($\theta = \pi/2$) diverge and initiate the hydrodynamic instability. In this case, chemotaxis can suppress the splay fluctuations for both infinite and finite systems of pullers and eventually stabilize the system. Note that parameters are chosen from the stable region of the phase diagram of spherical swimmers.

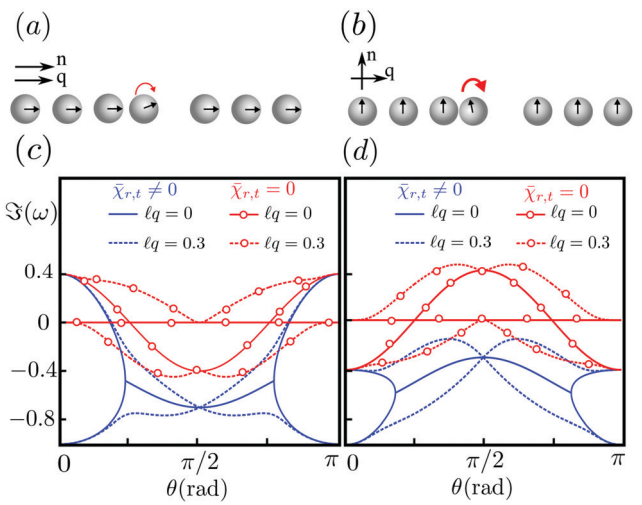

Fig. 3 (a and b) Demonstrate how chemotaxis tends to suppress both bend and splay distortions in a suspension of spherical swimmers. When a particle becomes misaligned with the polarization direction, due to its self-propulsion, a density fluctuation emerges and as shown in parts (a) and (b), that particle becomes closer to the swimmers in its left-hand-side. Then, it feels a stronger chemical sink in its left-hand-side and the chemotactic torque makes it aligned with polarization direction again. As we can see, restoring torque (shown by curved red arrow) is stronger for the case of splay fluctuations because density fluctuations are larger in this case. (c) and (d) show the growth rate, $\Im(\omega)$, as a function of wave angle θ in a suspension of nearly aligned pushers and pullers, respectively. In the absence of chemotaxis (red circle), bend distortions ($\theta = 0,\pi$) make pusher suspensions unstable, but for pullers, it is splay fluctuation ($\theta = \pi/2$) that initiates the instability. Effects due to chemotaxis, shown as blue lines, strongly (weakly) diminish splay (bend) fluctuations for infinite and finite systems. Numerical values are $a_2 = 8$, $|\Delta_p| = 0.2$, $\bar{\chi}_r = -0.6$ and $\bar{\chi}_t = -0.5$.

3.3 Effects due to elasticity

Elasticity that is identified by the bend and splay moduli K_b and K_s, is another interesting and relevant effect in systems with high density of particles and finite size that can suppress the fluctuations. To consider the elasticity, we note that the elastic free energy functional of the system can be written as:

$$F = \int F \mathrm{d}^3 r = \frac{1}{2}\int \left(K_s(\nabla \cdot \mathbf{n})^2 + K_b|\mathbf{n} \times \nabla \times \mathbf{n}|^2\right)\mathrm{d}^3 r. \quad (12)$$

As a result of this free energy, the following contribution should be added to the evolution of the polarization field:

$$\dot{\mathbf{n}}^{el} = -\Gamma_r^{-1}\left(\frac{\partial \mathcal{F}}{\partial \mathbf{n}} - \nabla \cdot \frac{\partial \mathcal{F}}{\partial \nabla \mathbf{n}}\right), \quad (13)$$

where Γ_r denotes a rotational friction coefficient. Including elasticity in our model, function $g(\theta)$ should be replaced by $g(\theta) = \Delta_p \cos 2\theta(1 + A\cos 2\theta) + \bar{\chi}_t - \bar{q}^2(\bar{K}_s \sin^2\theta + \bar{K}_b \cos^2\theta)$ in eqn (11). As shown in ref. 15, considering the case of spherical swimmers, elasticity introduces a length $L_b = \ell\sqrt{\bar{K}_b/\Delta_p}$ so that systems with smaller size ($L < L_b$) are stable against hydrodynamic fluctuations. Dimensionless moduli are defined as: $\bar{K}_{s,b} = (\ell/\omega_0\Gamma_r)K_{s,b}$. The presence of chemotaxis does not change this picture for a suspension of pushers but it enhances the threshold length-scale for a suspension of pullers to $L_s = \ell\sqrt{\bar{K}_s/(|\Delta_p| - |\bar{\chi}_t|)}$ (for $|\Delta_p| > |\bar{\chi}_t|$).

3.4 Effects due to friction with a substrate

In quasi two dimensional systems, friction with the substrate is another interesting and important factor in many experiments. It is shown that such friction can remove the instabilities by screening the long-range hydrodynamic interactions.[42] To study the dynamics of a suspension that is in contact with the substrate, we replace the Stokes equation by the following 2D effective equation:

$$-\Gamma \mathbf{u} - \nabla \Pi = \zeta_{2D}\nabla \cdot \mathbf{Q} + \Gamma' \mathbf{p}, \quad (14)$$

where $\Gamma(>0)$ and Γ' are two phenomenological friction coefficients for the fluid and swimmers, respectively.[43,44] Governing equations for $(\mathbf{p},\rho,c)$ remain unchanged except for some new re-scaled coefficients. Here and for 2D systems, density is replaced with σ_2, and also, we define $\zeta_{2D} = \eta\ell v_0 \Delta_p$. The coefficient $\Gamma' \sim \nu_0$ is

related to the activity of the system while Γ is a function of the fluid viscosity. Their exact forms depend on details of flow and polarization fields in the third direction. No-slip conditions for $\mathbf{u}$ force the parameter Γ to be always positive; however, the sign of Γ' can vary depending on the form by which the polarization depends on the perpendicular coordinate and also its boundary conditions.[36]

We assume in-plane system sizes to be larger than the system size in the perpendicular direction ($L \gg h$) and neglect the viscous damping in comparison with the frictional damping (note that due to this assumption, we cannot study the momentum conserving case by putting $\Gamma = 0$, here). Then, by substituting $\mathbf{u}$ and δc in the equations of density and polarization, linear equations are obtained:

$$\left\{i\bar{\omega} + iE\bar{q}\cos\theta + \bar{q}^2\left[\frac{2\bar{\chi}_t}{W} - \bar{D}\right]\right\}\delta\tilde{\sigma} - 2i\hat{\mathbf{q}}\cdot\delta\tilde{\mathbf{n}} = 0,$$
$$\left\{i\bar{\chi}_r\bar{q}^2\left[\frac{\gamma}{2W}\right] + \left[\frac{i\bar{q}^2E}{2} - \bar{q}^3\cos\theta\frac{\Delta_p}{\bar{\Gamma}}\right]A'\right\}\sin^2\theta\delta\tilde{\sigma}$$
$$+\left\{i\bar{\omega} - i\bar{q}\cos\theta\left[\frac{E(A'-2)}{2}+2\right] + \bar{q}^2\left[\frac{g(\theta)}{\bar{\Gamma}} - \bar{D}\right]\right\}\gamma\hat{\mathbf{q}}\cdot\delta\tilde{\mathbf{n}} = 0. \quad (15)$$

where $W = \sigma\partial_c K D_c^{-1}\ell^2 - i(\gamma_2 E/2)\mathrm{Pe}\bar{q}\cos\theta + \bar{q}^2$ and new dimensionless parameters are defined as $\bar{\Gamma} = \Gamma\ell^2/\eta$, $E = 2\Gamma'/(\nu_0\Gamma\ell^2)$, and $\gamma_2 = \sigma_2\ell^2$. To study the role of chemotaxis and friction in stabilizing the active suspension, the growth rate $\Im(\bar{\omega})$ is expanded in powers of perturbation wave vector up to $\bar{q}^2$. The numerical solution to the above equations reveals the stability diagram of the system and it is shown in Fig. 4. Here for the chemical reactions taking place on the surface of swimmers, we have considered the reaction-dominated regime. Stability of the polar state in the diffusion-dominated regime will be discussed at the end of this section.

In the absence of chemotaxis, friction can remove instability of both puller and pusher suspensions for sufficiently large values of $\Gamma(-\bar{\Gamma}_{\min} < \Delta_p < \bar{\Gamma}_{\max})$, when $\Gamma' < 0$. $-\bar{\Gamma}_{\min}$ and $\bar{\Gamma}_{\max}$ are denoted by two highlighted points on the vertical axis of Fig. 4(a) and (b). In this regime, $\bar{D}$ assigns maximum pusher strength in which the polar state can be stabilized without chemotaxis ($\Delta_p^{\text{critical}} \sim \bar{D}\bar{\Gamma}_{\max}$). In contrast, when $\Gamma' > 0$ frictional damping cannot stabilize any of the puller and pusher suspensions even by decreasing Δ_p or increasing $\bar{D}$. However, both regimes ($\Gamma' > 0$ and $\Gamma' < 0$) can be stabilized in the presence of chemotaxis as presented in Fig. 4(a) and 5. Parameters of these graphs are chosen as $\bar{\Gamma} = (\ell^2/\eta)\Gamma$, $\frac{D_c}{\nu_0\ell} = \frac{D_c}{\partial_c K} = \bar{D} = 1$ and $|E| = 2$, and the difference between them is in the sign of parameter Γ'.

As shown in Fig. 4 and 5, in the reaction-dominated regime chemotactic interaction can suppress hydrodynamic instabilities for both $\Gamma' > 0$ and $\Gamma' < 0$ cases. We should emphasize that, in the presence of a substrate, hydrodynamic interactions are screened and chemotaxis can affect the stability of the polar state even in the reaction-dominated regime in which chemotactic interaction does not mediate a long-range interaction between swimmers. To study the effects of Péclet number, the phase diagrams shown in Fig. 4(a) and (b) correspond to Pe = 1 and Pe = 0.2, respectively. In this regime and as it is seen from these phase diagrams, decreasing Péclet number Pe increases the stable regions.

In a regime in which the chemical equation is dominated by diffusion and for small Péclet numbers ($\mathrm{Pe} < 2\ell/(\gamma EL)$) chemotaxis appears in zeroth order in the expansion of the growth rate with respect to $\bar{q}$ (it remains finite as $\bar{q}$ goes to zero) and it can stabilize suspensions of both pullers and pushers. But, for large values of Péclet number, $\mathrm{Pe} > 2\ell/(\gamma EL)$ there is an instability in all directions. This instability originates from an

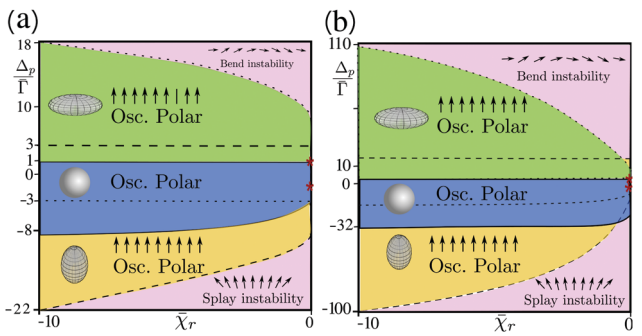

Fig. 4 Regions of stability for a momentum non-conserving suspension interacting with a substrate through friction coefficients $\bar{\Gamma}$ and $\Gamma' < 0$. On the vertical axes, two highlighted points specify an interval $-\bar{\Gamma}_{\min} < \Delta_p < \bar{\Gamma}_{\max}$, where the hydrodynamic screening stabilizes the system for $\Gamma' < 0$ and $\bar{\chi}_t = \bar{\chi}_r = 0$. With chemotaxis-assisted interaction, the stable region will grow. Here, we have set $E = -2$ and $\bar{\chi}_t = -2.5$ for two different values of the chemical Péclet number. (a) Corresponds to Pe = 1 and (b) corresponds to Pe = 0.2. Decreasing Pe increases the stable parts of the phase diagram.

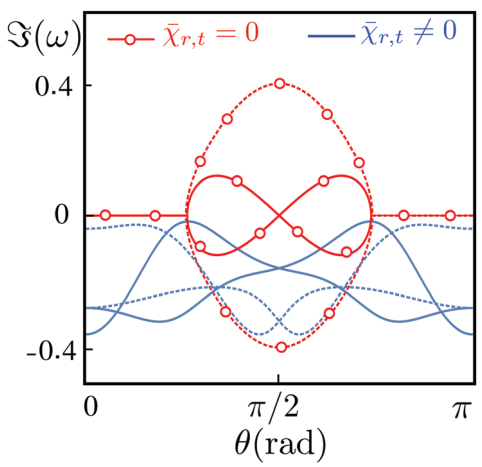

Fig. 5 Growth rate $\Im(\omega)$ as a function of wave angle θ in a suspension of nearly aligned oblate pushers (dashed lines) and prolate pullers (solid lines) in the presence of substrates. Here we consider $\Gamma' > 0$, where frictional damping cannot stabilize puller and pusher suspensions. In the absence of chemotaxis, both pusher and puller suspensions are unstable (red circle). Chemotactic interaction, shown as blue lines, diminishes fluctuations in both puller and pusher suspensions. Here, we have considered $\Gamma' > 0$ and we have set $|\Delta_p|/\bar{\Gamma} = 4$, $\bar{\chi}_r = -4.5$ and $\bar{q} = 0.2$.

advective term in the chemical equation and has a totally different origin from other instabilities previously observed in chemotactically interacting systems.[22,23,25]

4 Stability of the isotropic state

As mentioned before, for systems with small densities ($\rho_0 < \rho^*$), a homogenous steady state with uniform density and $\mathbf{p} = \mathbf{Q} = 0$ is expected to be observed. In this section, we study the stability of this isotropic state of swimmers in the bulk of the fluid and in the presence of chemotaxis. Here, in addition to density and polarization, the nematic order parameter is another relevant field, the fluctuations of which need to be considered. Denoting the fluctuations of nematic order by $\delta\tilde{\mathbf{Q}}$, linearized equations describing the long-wavelength fluctuations are given by:

$$-i\bar{\omega}\delta\tilde{\rho} = 2\bar{\chi}_t\delta\tilde{\rho} - 2i\gamma^{-1}\hat{\mathbf{q}}\cdot\delta\tilde{\mathbf{n}}, \tag{16a}$$

$$-i\bar{\omega}\hat{\mathbf{q}}\cdot\delta\tilde{\mathbf{n}} = 2\bar{D}\hat{\mathbf{q}}\cdot\delta\tilde{\mathbf{n}} + \frac{2}{3}\bar{\chi}_r\delta\tilde{\rho}, \tag{16b}$$

$$-i\bar{\omega}\delta\tilde{Q}_{\mathrm{d}} = -\frac{8}{15}i\gamma^{-1}\hat{\mathbf{q}}\cdot\delta\tilde{\mathbf{n}} - 6\bar{D}_r\delta\tilde{Q}_{\mathrm{d}}, \tag{16c}$$

$$-i\bar{\omega}\delta\tilde{Q}_{\mathrm{o}} = \left(\frac{4}{5}A\Delta_{\mathrm{p}} - 6\bar{D}_r\right)\delta\tilde{Q}_{\mathrm{o}}, \tag{16d}$$

where diagonal and off-diagonal elements of the nematic tensor are defined by $\delta\tilde{Q}_{\mathrm{d}} = \hat{\mathbf{q}}\cdot\delta\tilde{\mathbf{Q}}\cdot\hat{\mathbf{q}}$ and $\delta\tilde{Q}_{\mathrm{o}} = (\mathbf{I} - \hat{\mathbf{q}}\hat{\mathbf{q}})\cdot\delta\tilde{\mathbf{Q}}\cdot\hat{\mathbf{q}}$, respectively. As seen from the above equations, evolution of $\delta\tilde{Q}_{\mathrm{o}}$ is not coupled to other fields and hydrodynamic effects are entered through this field. As a result, chemotaxis and hydrodynamics appear in separate modes and none of these modes can affect instabilities generated by the other.

For the diffusion-dominated regime, linearizing the dynamical equations leads to the following modes for the fluctuations at $\bar{q} = 0$:

$$\bar{\omega} = \left\{ i\bar{\chi}_t - i\bar{D} \pm i\left(\frac{2}{3}\bar{\chi}_r + (\bar{\chi}_t + \bar{D})^2\right)^{\frac{1}{2}}, \frac{4i}{5}A\Delta_{\mathrm{p}} - 6i\bar{D}_r \right\},$$

Stability of an isotropic suspension of swimmers depends not only on their type (pusher or puller), but also on their shape through parameter A. In the absence of chemotaxis and for $A\Delta_{\mathrm{p}} > 15\bar{D}_r/2$, the isotropic state is unstable both for a suspension of pushers ($\Delta_{\mathrm{p}} > 0$) with $A > 0$ and for pullers ($\Delta_{\mathrm{p}} < 0$) with $A < 0$.[39,41] An isotropic suspension of spherical swimmers ($A = 0$) is always stable. As one can see from the above equations, modes associated with hydrodynamics and chemotaxis are independent and chemotaxis is not able to remove the hydrodynamic instabilities. Taking into account the stability criterion for both hydrodynamic and chemotaxis parts, we see that for $A\Delta_{\mathrm{p}} < 15\bar{D}_r/2$, a stable isotropic state can be observed under the condition $\bar{\chi}_t < \bar{D}$ and $\bar{\chi}_r < -6\bar{D}\bar{\chi}_t$.

Extending all of the above results for the reaction-dominated regime, we see that the chemotaxis mechanism does not have any strong effect on the phase portrait of both polar and isotropic momentum conserving suspensions as q goes to zero. In this regime, any local decrease in chemical molecules does not have enough time to diffuse and propagate to the position of other swimmers and subsequently chemotaxis is not able to remove hydrodynamic instabilities.

5 Concluding remarks

In this article, we have studied the role of chemotactic interaction in both wet (bulk 3D) and dry (quasi 2D) active systems and have shown that for both pushers and pullers, chemotaxis can suppress the fluctuations and stabilize the polar state. To consider the physics of chemotaxis, we benefited from phenomenological theories. In the phenomenological level, two dimensionless parameters $\bar{\chi}_t$ and $\bar{\chi}_r$ are used. It would be constructive to see how the results presented here can be of relevance to physical systems. To this end, we may estimate the range of chemotactic coefficients in micron scale systems. In this regard, we note that the chemotactic velocity has the same order of magnitude as the swimming speed; thus $\chi_t \sim v_0\ell/c$. For a swimmer with $v_0 = 50\ \mu\mathrm{m\ s^{-1}}$ and $\ell = 5\ \mu\mathrm{m}$, moving in a 10 μM concentration of food molecules with $D_c \sim 5 \times 10^{-10}\ \mathrm{m^2\ s^{-1}}$, we can estimate the dimensionless chemotactic coefficients as: $\bar{\chi}_t \sim \bar{\chi}_r \sim \mathcal{O}(1)$. Here we have used $K_0 \sim 10^3\ \mathrm{s^{-1}}$ and $\rho_0 \sim 10^{16}\ \mathrm{m^{-3}}$. This estimation shows that our choice of parameters in Fig. 1 can cover real systems. Thus for typical systems that are accessible in experiments, the proposed mechanism can successfully work.

In summary, we have shown that fluctuation suppression due to chemotaxis in the bulk of a fluid is much stronger for pullers. This can eventually develop a stable region in their phase diagram for various geometries of swimmers. However, for pushers in bulk fluid, chemotaxis can only stabilize suspensions of disk-shaped swimmers. In the presence of a substrate and for small Péclet numbers, chemotactic mediated interaction in the diffusion-dominated regime can stabilize both puller and pusher suspensions with different geometries. In the case of large Péclet number, chemotactic interaction in the reaction-dominated regime can stabilize hydrodynamic fluctuations and develop stable regions in the phase diagram.

Conflicts of interest

There are no conflicts to declare.

Acknowledgements

Helpful discussion with S. Ramaswamy is gratefully acknowledged.

References

1 T. Vicsek and A. Zafeiris, *Phys. Rep.*, 2012, **517**, 71–140.
2 M. C. Marchetti, J. F. Joanny, S. Ramaswamy, T. B. Liverpool, J. Prost, M. Rao and R. A. Simha, *Rev. Mod. Phys.*, 2013, **85**, 1143–1189.
3 D. Saintillan and M. J. Shelley, *Phys. Fluids*, 2008, **20**, 123304.

4 S. Ramaswamy, *Annu. Rev. Condens. Matter Phys.*, 2010, **1**, 323–345.
5 F. Jülicher, K. Kruse, J. Prost and J.-F. Joanny, *Phys. Rep.*, 2007, **449**, 3–28.
6 R. A. Simha and S. Ramaswamy, *Phys. Rev. Lett.*, 2002, **89**, 058101.
7 T. Bickel, G. Zecua and A. Würger, *Phys. Rev. E: Stat., Nonlinear, Soft Matter Phys.*, 2014, **89**, 050303.
8 T. Vicsek, A. Czirók, E. Ben-Jacob, I. Cohen and O. Shochet, *Phys. Rev. Lett.*, 1995, **75**, 1226–1229.
9 H. M. López, J. Gachelin, C. Douarche, H. Auradou and E. Clément, *Phys. Rev. Lett.*, 2015, **115**, 028301.
10 J. Urzay, A. Doostmohammadi and J. M. Yeomans, *J. Fluid Mech.*, 2017, **822**, 762–773.
11 S. Rafa, L. Jibuti and P. Peyla, *Phys. Rev. Lett.*, 2010, **104**, 098102.
12 J. Prost, F. Jülicher and J.-F. Joanny, *Nat. Phys.*, 2015, **11**, 111–117.
13 M. Moradi and A. Najafi, *EPL*, 2015, **109**, 24001.
14 S. Ramaswamy, *J. Stat. Mech.: Theory Exp.*, 2017, 054002.
15 S. Ramaswamy and M. Rao, *New J. Phys.*, 2007, **9**, 423.
16 R. Voituriez, J. F. Joanny and J. Prost, *EPL*, 2005, **70**(3), 404.
17 M. Leoni and T. B. Liverpool, *Phys. Rev. Lett.*, 2010, **105**, 238102.
18 J. Adler, *Science*, 1966, **153**, 708–716.
19 S. Saha, R. Golestanian and S. Ramaswamy, *Phys. Rev. E: Stat., Nonlinear, Soft Matter Phys.*, 2014, **89**, 062316.
20 N. Desai and A. M. Ardekani, *Soft Matter*, 2017, **13**, 6033–6050.
21 I. Theurkauff, C. Cottin-Bizonne, J. Palacci, C. Ybert and L. Bocquet, *Phys. Rev. Lett.*, 2012, **108**, 268303.
22 E. F. Keller and L. A. Segel, *J. Theor. Biol.*, 1970, **26**, 399–415.
23 E. F. Keller and L. A. Segel, *J. Theor. Biol.*, 1971, **30**, 225–234.
24 C. Jin, C. Krüger and C. C. Maass, *Proc. Natl. Acad. Sci. U. S. A.*, 2017, **114**, 5089–5094.
25 B. Liebchen, D. Marenduzzo and M. E. Cates, *Phys. Rev. Lett.*, 2017, **118**, 268001.
26 T. Bickel, G. Zecua and A. Wuerger, *Phys. Rev. E: Stat., Nonlinear, Soft Matter Phys.*, 2014, **89**, 050303.
27 E. Lushi, R. E. Goldstein and M. J. Shelley, *Phys. Rev. E: Stat., Nonlinear, Soft Matter Phys.*, 2012, **86**, 040902.
28 J. L. Anderson, *Annu. Rev. Fluid Mech.*, 1989, **21**, 61–99.
29 O. Pohl and H. Stark, *Phys. Rev. Lett.*, 2014, **112**, 238303.
30 G. Jeffery, *Proc. R. Soc. London, Ser. A*, 1922, **102**, 161–179.
31 M. Farzin, K. Ronasi and A. Najafi, *Phys. Rev. E: Stat., Nonlinear, Soft Matter Phys.*, 2012, **85**, 061914.
32 C. M. Pooley, G. P. Alexander and J. M. Yeomans, *Phys. Rev. Lett.*, 2007, **99**, 228103.
33 H. Behmadi, Z. Fazli and A. Najafi, *J. Phys.: Condens. Matter*, 2017, **29**, 115102.
34 Z. Fazli and A. Najafi, *J. Stat. Mech.: Theory Exp.*, 2018, **2018**(2), 023201.
35 K. A. Johnson and R. S. Goody, *Biochemistry*, 2011, **50**, 8264–8269.
36 A. Maitra, P. Srivastava, M. C. Marchetti, J. Lintuvuori, S. Ramaswamy and M. Lenz, *Proc. Natl. Acad. Sci. U. S. A.*, 2018, **115**(27), 6934–6939.
37 P. A. Spiro, J. S. Parkinson and H. G. Othmer, *Proc. Natl. Acad. Sci. U. S. A.*, 1997, **94**(14), 7263–7268.
38 C. V. Rao, J. R. Kirby and A. P. Arkin, *PLoS Biol.*, 2004, **2**(2), 0239–0252.
39 D. Saintillan and M. J. Shelley, *Phys. Rev. Lett.*, 2008, **100**, 178103.
40 A. Baskaran and M. C. Marchetti, *Phys. Rev. E: Stat., Nonlinear, Soft Matter Phys.*, 2008, **77**, 011920.
41 A. Baskaran and M. C. Marchetti, *Proc. Natl. Acad. Sci. U. S. A.*, 2009, **106**, 15567–15572.
42 A. Doostmohammadi, M. F. Adamer, S. P. Thampi and J. M. Yeomans, *Nat. Commun.*, 2016, **7**, 10557.
43 I. S. Aranson, A. Sokolov, J. O. Kessler and R. E. Goldstein, *Phys. Rev. E: Stat., Nonlinear, Soft Matter Phys.*, 2007, **75**, 040901.
44 G. Luca and M. C. Marchetti, *Soft Matter*, 2012, **8**, 129–139.